24th INTERNATIONAL CONGRESS ON SOUND AND VIBRATION
23–27 July 2017, London

RESPONSE PREDICTION OF A MECHANICAL SYSTEM WITH VIRTUAL BOUNDARY CONDITIONS BASED ON THE BLOCKED TRANSFER FUNCTION METHOD

Songbin Tan, Hao Xu, Fusheng Sui

Key Laboratory of Noise and Vibration Research, Institute of Acoustics, University of Chinese Academy of Sciences, Beijing, China
Email: sui@mail.ioa.ac.com

In this paper, a method to predict the response of mechanical system under virtual boundary conditions is presented in the framework of global transfer direct transfer (GTDT) method. The proposed method is capable of avoiding the inconvenience of implementing boundary conditions when measuring the response. Meanwhile, in order to deal with multiple points in the object region, the direct transfer functions (DTFs) in GTDT is extended to the single input to multiple outputs transfer functions named as blocked transfer functions (BTFs). At last the finite element analysis simulation of a plate is formed. And the prediction of the proposed method agrees well with the results under practical boundary conditions.
Keywords: Response prediction, blocked transfer function

1. Introduction

In the late 1970s, transmission path analysis (TPA) techniques were first developed to determine vibro-acoustic transfer paths in a mechanical system [1, 2]. Over time, several families of TPA have been proposed: classical TPA, component based TPA, transmissibility based TPA [3].

Classical TPA is first proposed and has been improved into different variants [2,4,5]. The family of classical TPA is intended to identify transfer path contribution by determined the interface force between the active part and passive part of the tested system. Different variants of classical TPA are defined according to how interface force is obtained. Component based TPA [6-8] characterizes the source excitation by a set of equivalent forces or velocities, which will not be affected by modifications of other parts of the system. Both of the two families of TPA require dismounting of the active part from the passive side. On the contrary, transmissibility based TPA conducts measurements on the assembled system, avoiding the inconvenience of the dismounting operations. The most popular and respective method of transmissibility based TPA is operational TPA [9-12], which conduct all measurements only in the operating condition.

A method named as global transfer direct transfer (GTDT) method was first proposed by Magrans in 1981 [12], further explored by Guasch [13-15] and later put into practice as the advanced transfer path analysis (ATPA). This method uses transmissibility concept in the framework of classical TPA, consuming less time than classical TPA and being more accurate than OTPA. It proposed two concepts: global transfer function (GTF) and direct transfer function (DTF), which are easily measurable quantity and desired path-blocking quantity, respectively.

This paper extends the DTF to a new concept, blocked transfer function (BTF), which stands for the quotient between the input and outputs when some selected points are blocked. Note that BTF is a single input to multiple outputs transfer function while DTF is a single to single one. And the DTF and BTF can be calculated by the GTF matrixes, which can be measured without changing the physical states of the mechanical system. Hence it is capable to calculate the transmissibility of the

source to multiple targets or even the whole system under a virtual boundary condition. The virtual boundary condition mentioned here means the (blocked) boundary condition under which we want to measure the response while it is not really exists. When engineers expect to know the response of a desired zone of a system with blocked boundary conditions, they may suffer the inconvenience to implement them. The method proposed in this paper using BTF will be a good choice to deal with this problem. It is not necessary to implement real boundary conditions while engineers could set up a series of sensors instead.

This paper is organized as follows. In section 2, the derivation of BTF from the framework of GTDT method is shown, and the formulation of BTF calculated from GTF is presented. In section 3, a finite element analysis simulation of a rectangle plate with irregular boundary conditions is formed, as a simple numerical example. Finally, conclusions are worked out in section 4.

2. Theory

2.1 Basic Concepts of the GTDT method

As quoted in In the framework of global transfer direct transfer (GTDT) TPA method [12], the global transfer function (GTF) T_{ij}^{G} from subsystem i and j is defined as the quotient between the signal at j, $s_j(\omega)$, and the signal at i, $s_i(\omega)$, when there is only one non-zero and independent external excitation, $f_i^{ext}(\omega)$, applied to i which has been transmitted to j via a global path:

$$T_{ij}^{G}(\omega)=\frac{s_j(\omega)}{s_i(\omega)} \quad with \quad f^{ext}(\omega)=(0,\cdots,0,\, f_i^{ext}(\omega),0,\cdots,0)^T \tag{1}$$

And the direct transfer function (DTF) T_{ij}^{D} from subsystem i to j is defined as the quotient between the signal at j, $s_j(\omega)$, and the signal at i, $s_i(\omega)$, when a non-zero and independent external excitation, $f_i^{ext}(\omega)$, applied to i that has been transmitted to j via direct path, i.e., all other signals $s_k(\omega)$, with $k\neq i, j$ remain zero:

$$T_{ij}^{D}(\omega)=\frac{s_j(\omega)}{s_i(\omega)} \quad with \quad s_k(\omega)=0, \quad \forall k\neq i, j \tag{2}$$

As a consequence, the signal s_k is equal to the sum of the contribution of all the other points:

$$s_k=\sum_{\substack{1\\ j\neq k}}^{n} T_{jk}^{D} s_j \tag{3}$$

2.2 Derivation of blocked transfer function

First we consider a general N-dimensional system network in which only m subsystems are considered in the framework of GTDT method. We define the m subsystems considered as a gather M, and the $n-m$ subsystems left as a gather L.

If subsystem i is excited, the signal of subsystem k $(k\neq i)$ can be expressed as

$$s_k=\sum_{\substack{1\\ j\neq k}}^{m} \hat{T}_{jk}^{D} s_j \tag{4}$$

Note that $\hat{T}_{jk}^{D}$, the DTF when only m subsystems are of interest, is not equal to T_{jk}^{D}, the DTF when all of the n subsystems are taken into consideration.

When all the subsystems of M are somehow blocked except subsystem i and k which are respectively the input and output point, the signal of the subsystem k will be

$$s_k^B = T_{ik}^D s_i^B + \sum_{j=m+1}^{n} T_{jk}^D s_j^B \tag{5}$$

Thus

$$T_{ik}^B = T_{ik}^D + \sum_{j=m+1}^{n} T_{jk}^D T_{ij}^B \tag{6}$$

where $T_{ij}^B = \frac{s_j^B}{s_i^B}$ is the GTF from i to j in the blocked system.

As the definition of the DTF, $\hat{T}_{ik}^D$ should be equal to T_{ik}^B. Therefore Eq. (4)will change to

$$s_k = \sum_{\substack{1 \\ j \neq k}}^{m} T_{jk}^B s_j \tag{7}$$

Substitute Eq. (6)into Eq. (7)

$$s_k = \sum_{\substack{1 \\ j \neq k}}^{m} (T_{jk}^D + \sum_{l=m+1}^{n} T_{lk}^D T_{jl}^B) s_j$$

$$= \sum_{\substack{1 \\ j \neq k}}^{n} T_{jk}^D s_j + \sum_{\substack{1 \\ j \neq k}}^{m} \sum_{l=m+1}^{n} T_{lk}^D T_{jl}^B s_j - \sum_{l=m+1}^{n} T_{lk}^D s_l \tag{8}$$

$$= s_k + \sum_{\substack{1 \\ j \neq k}}^{m} \sum_{l=m+1}^{n} T_{lk}^D T_{jl}^B s_j - \sum_{l=m+1}^{n} T_{lk}^D s_l$$

Note that Eq. (3)has been used in the third step.

As a result, it will not be self-consistent except for

$$\sum_{\substack{1 \\ j \neq k}}^{m} \sum_{l=m+1}^{n} T_{lk}^D T_{jl}^B s_j = \sum_{l=m+1}^{n} T_{lk}^D s_l \tag{9}$$

which can be rewritten as

$$\sum_{l=m+1}^{n} (\sum_{\substack{1 \\ j \neq k}}^{m} T_{jl}^B s_j) T_{lk}^D = \sum_{l=m+1}^{n} s_l T_{lk}^D \tag{10}$$

It follows that

$$s_l = \sum_{\substack{1 \\ j \neq k}}^{m} T_{jl}^B s_j \quad with \quad l = m+1, m+2, \cdots, n \tag{11}$$

It reveals that s_l, the signal of subsystem l, included in the gather L, can be expressed as the sum of the contributions of the m considered subsystems. From the definition of GTF, it becomes

$$T_{il}^G = \sum_{\substack{1 \\ j \neq k}}^{m} T_{jl}^B T_{ij}^G \quad with \quad l = m+1, m+2, \cdots n \tag{12}$$

On the other hand, combine Eq. (11)with Eq. (7), we can draw a conclusion that subsystem l acts a role similar to the receiving subsystem k. Eq. (12) then becomes

$$T_{il}^G = \sum_{\substack{1 \\ j \neq k}}^{m} T_{jl}^B T_{ij}^G \quad with \quad l = m+1, m+2, \cdots, n \tag{13}$$

Note that subsystem k can be included in gather L.

Therefore the matrix equation can be built as

$$\begin{pmatrix} T^G_{1,m+1} & T^G_{1,m+2} & \cdots & T^G_{1n} \\ T^G_{2,m+1} & T^G_{2,m+2} & \cdots & T^G_{2n} \\ \vdots & \vdots & \ddots & \vdots \\ T^G_{m,m+1} & T^G_{m,m+2} & \cdots & T^G_{mn} \end{pmatrix} = \begin{pmatrix} T^G_{11} & T^G_{12} & \cdots & T^G_{1m} \\ T^G_{21} & T^G_{22} & \cdots & T^G_{2m} \\ \vdots & \vdots & \ddots & \vdots \\ T^G_{m1} & T^G_{m2} & \cdots & T^G_{mm} \end{pmatrix} \begin{pmatrix} T^B_{1,m+1} & T^B_{1,m+2} & \cdots & T^B_{1n} \\ T^B_{2,m+1} & T^B_{2,m+2} & \cdots & T^B_{2n} \\ \vdots & \vdots & \ddots & \vdots \\ T^B_{m,m+1} & T^B_{m,m+2} & \cdots & T^B_{mn} \end{pmatrix} \tag{14}$$

Or

$$\mathbf{T}^{\mathbf{G}}_{m\times(n-m)} = \mathbf{T}^{\mathbf{G}}_{m\times m}\mathbf{T}^{\mathbf{B}}_{m\times(n-m)} \tag{15}$$

if $\det(\mathbf{T}^{\mathbf{G}}_{m\times m}) \neq 0$, it will be

$$\mathbf{T}^{\mathbf{B}}_{m\times(n-m)} = (\mathbf{T}^{\mathbf{G}}_{m\times m})^{-1}\mathbf{T}^{\mathbf{G}}_{m\times(n-m)} \tag{16}$$

Where $\mathbf{T}^{\mathbf{B}}_{m\times(n-m)} = \begin{pmatrix} T^B_{1,m+1} & T^B_{1,m+2} & \cdots & T^B_{1n} \\ T^B_{2,m+1} & T^B_{2,m+2} & \cdots & T^B_{2n} \\ \vdots & \vdots & \ddots & \vdots \\ T^B_{m,m+1} & T^B_{m,m+2} & \cdots & T^B_{mn} \end{pmatrix}$. Now define T^B_{il}, an element of $\mathbf{T}^{\mathbf{B}}_{m\times(n-m)}$, as the blocked transfer function from subsystem i included in M to subsystem l included in L. Note that "blocked" means the signal of all the subsystems in M except the input subsystem j are forced to zero.

Therefore, the DTF (Direct Transfer Function) of GTDT method is expanded to the concept BTF (Blocked Transfer Function).

2.3 Differences and connection among GTF, DTF and BTF

Now the N-dimensional system can be divided into three parts: the input subsystem i, the blocked gather B within $m-1$ subsystems and the output gather S within $n-m$ subsystems. Note that the gather M mentioned in last subsection contains i and B, and L equals to S.Then BTFs can be described as follow: the transmissibility from a single input subsystem i to the subsystems in output gather S when all the subsystems in gather B are blocked. To calculate the BTFs, one should excite the subsystems in gather M respectively and record the signal1 of all the subsystems. When subsystem i $(i=1,2,\cdots,m)$ is excited, the GTFs will be obtained as the elements of the matrixes of right hand side of Eq.(16). Hence, BTFs, the left hand side of Eq. (16), can be obtained.

When the blocked gather M increases to $n-2$ elements, the BTFs change to DTFs as all subsystems of the N-dimensional system blocked except the input and output subsystem. When the blocked gather M reduces to one element, the BTFs turn into GTFs as there is no any subsystem blocked. The sketch maps of GTFs, DTFs and BTFs are shown in Fig.1a, Fig.1b and Fig1.c. Consequently, the BTFs are the intermediate quantity between GTFs and DTFs, or we can regard the GTFs and DTFs as special examples of BTFs.

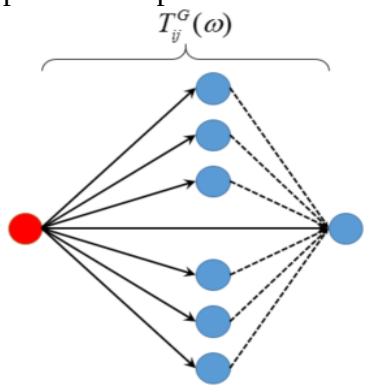

Fig.1a

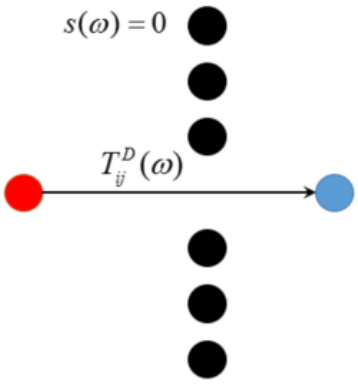

Fig.1b

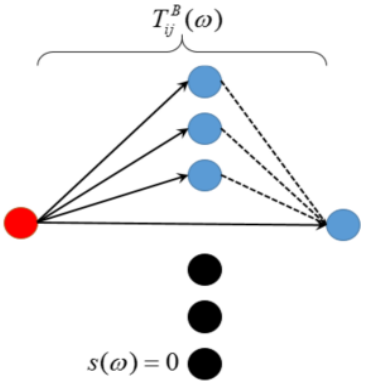

Fig.1c

3. Application of BTF

Engineers may expect to measure the response of a series of subsystems S with the boundary condition that some other subsystems M are blocked when one points i is excited, while it is impossible or inconvenient to implement the boundary condition. However, they can use the BTF concept mentioned above to deal with it. In a mechanical system,

3.1 Numerical experiment

A numerical example of a clamped rectangle aluminum plate is formed by the LMS Virtual.lab 13, which is a finite element analysis software. The plate is excited by a point harmonic force. And the prediction of the response of it under two kinds of virtual boundary conditions (Fig.2 and Fig.3) is worked out. The parameters of the aluminum plate is shown in Table 1.

Table 1: Parameters of the plate

Size（mm）	900×600×2
Young modulus（N/m2）	7.0×10^{7}
Poisson ratio	0.27
density（kg/m3）	2700

As shown in Fig.2 and Fig.3 seen blow, the white triangle, the red points and the rectangle are the input point, blocked points and output zone, respectively. Fig.2 shows the FEA model in situation 1. In this situation, the four sides of the aluminum plate are clamped originally and the virtual boundary condition added to this model is in-plate (the blocked points in the figure). However, Fig.3 shows another situation. In situation 2 shown by Fig.3, only three sides are clamped, and the virtual boundary condition is added on the remained side, as we want to predict the response of the plate with four sides clamped.

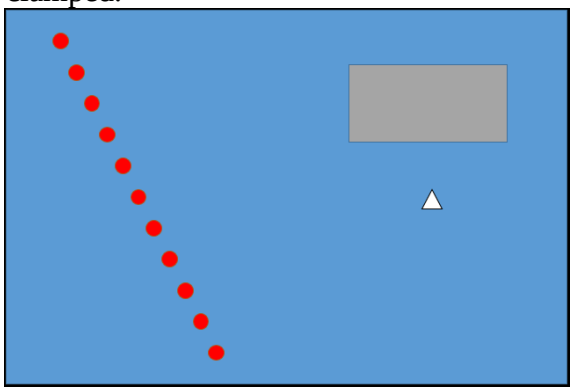

Fig.2: FEA model in situation 1

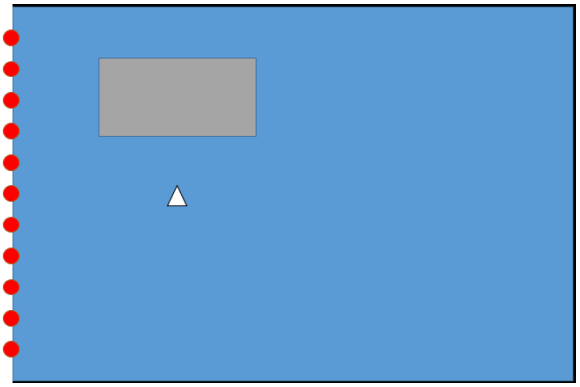

Fig.3: FEA model in situation 2

The numerical experiment is conducted as follow. First, excite the input points and all the blocked points, respectively. Meanwhile measure the response of all the interest points and form the m-rows and n-columns global transfer function matrix $\mathbf{T}^{\mathbf{G}}_{m\times n}$. Then divide this matrix into two parts: the matrix $\mathbf{T}^{\mathbf{G}}_{m\times m}$ contains first m columns and $\mathbf{T}^{\mathbf{G}}_{m\times(n-m)}$ contains the rest. Finally, substitute them into Eq. (16) and the blocked transfer function matrix $\mathbf{T}^{\mathbf{B}}_{m\times(n-m)}$ will be built. Note that the elements of the first row are the transfer functions between the input point i and the output points gather S, when all the points in blocked gather B are fixed. As a consequence, the response of gather B can be easily got from $\mathbf{T}^{\mathbf{B}}_{m\times(n-m)}$, when the system is excited by the source with constant velocity.

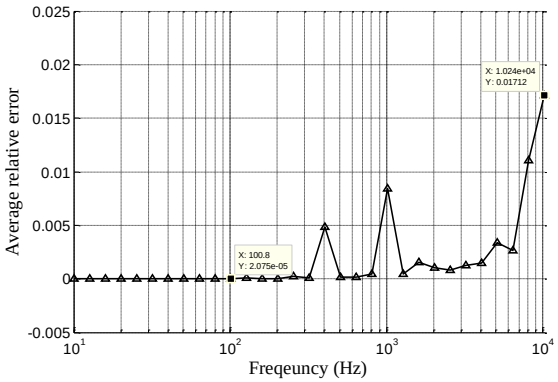

Fig.4: Average relative error of situation 1, from 10Hz to 10240Hz, 1/3 Octave.

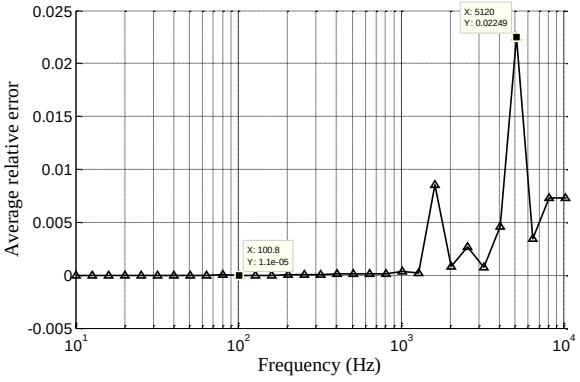

Fig.5: Average relative error of situation 2, from 10Hz to 10240Hz, 1/3 Octave.

3.2 Results and discussion

A comparison between the calculated blocked function T_{ij}^{B} and the measured transfer functions under real boundary condition is shown in this subsection. And the One-third octave band spectrum from 10Hz to 10240Hz of average relative error between them in the two situations mentioned above is given in Fig.4 and Fig.5.

The results show that the average relative error at low frequency band is very small, for example, the average relative error at 100Hz is around 0.001%. However at high frequency band it rise to a higher level, especially at some specific frequency. In situation 1 the highest value 1.71% appears at 10240 Hz and in situation 2 the highest value 2.25% appears at 5120 Hz. All the others are below 1% and most are below 0.5%, which means the prediction agrees well with the true value.

More details of the bad point are analysed as follow. Fig.6 shows the curve of the prediction and true value of all output points at 5120 Hz in situation 2. Fig.7 shows the relative error of all output points in the same case. It can be seen that there are several abnormal high value points in Fig.7. And the value of corresponding points in Fig.6 are nearly 0, such as the 98th point. So that these points should be wiped off to evaluate the results more accurately. Fig.6 and Fig.7 show the comparison of the average relative error before and after wiping off the bad points. After wiping off these points, the average relative error at high frequency decreases but is still higher than the value at low frequency. There may be two possible reasons: 1, at high frequency, as the number of vibration modes increase, the response of the plate is much more complicated and the gradient is larger; 2, the number of the mesh in one wavelength decreases as the frequency increases, leading to less accuracy. Consequently, a new simulation with smaller model or larger mesh density will be more accurate.

Fig.10 shows the comparison of average relative error between two models with different size of the plate. While Fig.11 shows the comparison of average relative error between two models with different size of the mesh. To make the comparison clearer, the average relative error are shown with the unit dB in these figures. Fig.10 shows that at mid-high frequency the average relative error of smaller size model is much less than the larger one. As the average relative error of both are too small to influence the result at low frequency, we can draw a conclusion that the first reason of inaccuracy metioned in last paragragh is right. Fig.11 shows that at most of the frequency points of the FEA model with 2mm mesh are a little smaller than the model with 5mm mesh, and at the extraordinary high point the difference is much more obvious. The second reason of inaccuracy is also proved to be right.

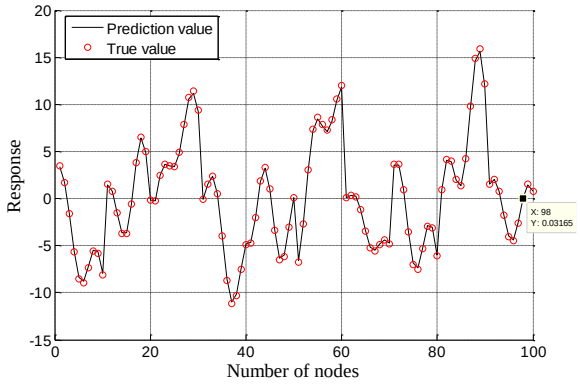

Fig.6: Prediction and true value of all output points at 5120 Hz in situation 2

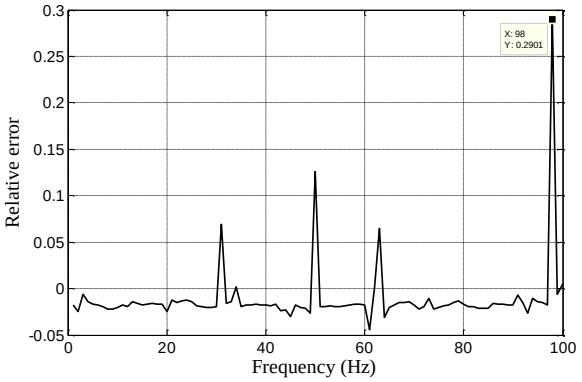

Fig.7: Relative error of all output points at 5120 Hz in situation 2

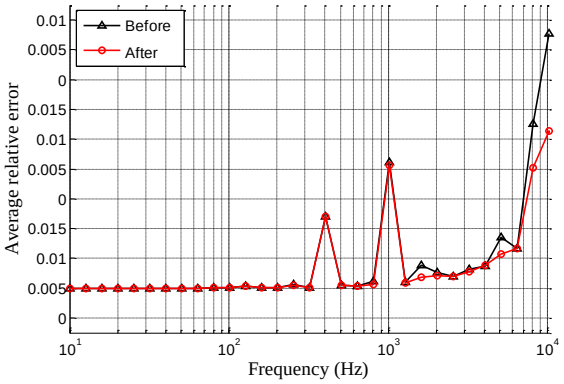

Fig.8: Average relative error of situation 1 from 10Hz to 10240Hz, 1/3 Octave. Before: original data; After: data after wiping off bad points

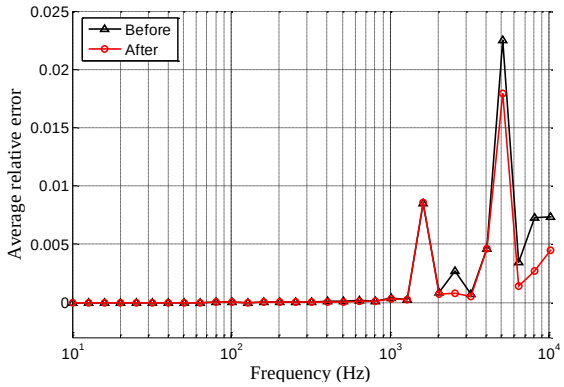

Fig.9: Average relative error of situation 2 from 10Hz to 10240Hz, 1/3 Octave. Before: original data; After: data after wiping off bad points

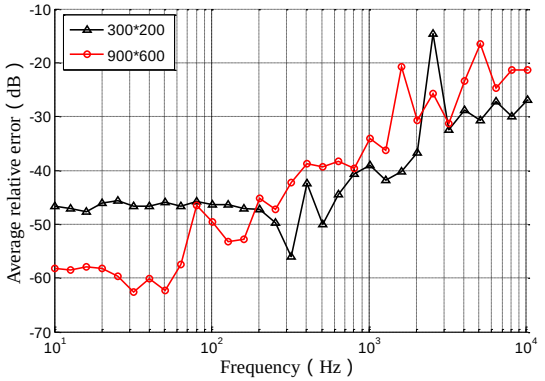

Fig.10 Comparison of average relative error between two models with different size of the plate.

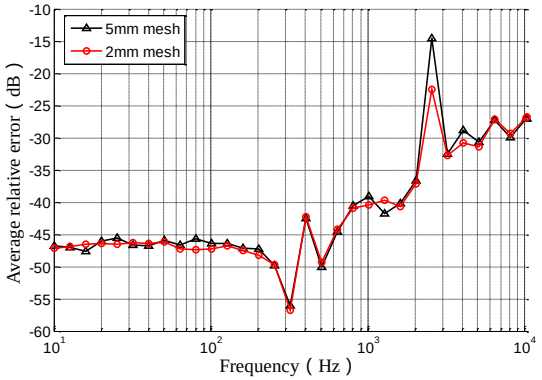

Fig.11 comparison of average relative error between two models with different size of the mesh

4. Conclusion

In this paper, the response prediction of a clamped plate with virtual boundary conditions has been studied using the blocked transfer function method. The blocked transfer function method is developed in this paper from the GTDT method, as a single input to multiple outputs method instead

of the single to single one. The derivation of the definitions and formulas of the proposed method is also shown.

The prediction capabilities of the method when used in a clamped rectangle aluminum plate have been also analysed. It has been shown that the prediction value agrees very well with the true one at low frequency, while the average relative error increases to a higher level at high frequency range. However, after wiping off some near-zero points, the average relative error partly decreases. At last, different FEA models are analysed to find the cause of the inaccuracy.

References

[1] Verheij J W. Measuring sound transfer through resilient mountings for separate excitation with orthogonal translations and rotations[J]. 1980.

[2] Verheij J W. Multi-path sound transfer from resiliently mounted shipboard machinery: experimental methods for analyzing and improving noise control /[D]. 1982.

[3] Seijs M V V D, Klerk D D, Rixen D J. General framework for transfer path analysis: History, theory and classification of techniques ☆[J]. *Mechanical Systems & Signal Processing*, 2015, s 68–69:217-244.

[4] Barten E, Seijs M V V D, Klerk D D. A Complex Power Approach to Characterise Joints in Experimental Dynamic Substructuring[J]. 2014, 42:281-296.

[5] Powell R E, Seering W. Multichannel Structural Inverse Filtering[J]. *Journal of Vibration & Acoustics*, 1984, 106(1):22-28.

[6] Bonhoff H A, Petersson B A. The significance of cross‐order terms in interface mobilities for structure‐borne sound source characterization[J]. *Journal of Sound & Vibration*, 2010, 322(1–2):241-254.

[7] Janssens M H A, Verheij J W, Thompson D J. The use of an equivalent forces method for the experimental quantification of structural sound transmission in ships[j]. *Journal of Sound & Vibration*, 1999, 226(2):305-328.

[8] Klerk D. Dynamic Response Characterization of Complex Systems through Operational Identification and Dynamic Substructuring[J]. Tu Delft, 2009.

[9] Klerk D D, Ossipov A. Operational transfer path analysis: Theory, guidelines and tire noise application[J]. *Mechanical Systems & Signal Processing*, 2010, 24(7):1950–1962.

[10] Gajdatsy P, Janssens K, Desmet W, et al. Application of the transmissibility concept in transfer path analysis[J]. *Mechanical Systems & Signal Processing*, 2010, 24(7):1963-1976.

[11] Lohrmann M. Operational transfer path analysis: Comparison with conventional methods[J]. *Journal of the Acoustical Society of America*, 2008, 123(5):3534.

[12] Magrans F X. Method of measuring transmission paths[J]. *Journal of Sound & Vibration*, 1981, 74(3):321-330.

[13] Guasch O, Magrans F X. The Global Transfer Direct Transfer method applied to a finite simply supported elastic beam[J]. *Journal of Sound & Vibration*, 2004, 276(276):335-359.

[14] Guasch O. Direct transfer functions and path blocking in a discrete mechanical system[J]. *Journal of Sound & Vibration*, 2009, 321(3–5):854-874.

[15] Guasch O, Garc á C, JovÉ J, et al. Experimental validation of the direct transmissibility approach to classical transfer path analysis on a mechanical setup[J]. *Mechanical Systems & Signal Processing*, 2013, 37(37):353–369.

ACKNOWLEDGEMENTS

This work was supported by the National Key technologies Research &Development program under Grant No. 2016YFC0801702 and National key Basic Research Program of China (973 Program) under Grant No. 2013CB632905.